JOURNAL OF VIROLOGY, Apr. 1996, p. 2107–2115 Vol. 70, No. 4
0022-538X/96/$04.00+0

The Turnip Yellow Mosaic Virus tRNA-Like Structure Cannot Be Replaced by Generic tRNA-Like Elements or by Heterologous 3′ Untranslated Regions Known To Enhance mRNA Expression and Stability†

JAMES M. SKUZESKI,[1] CONNIE S. BOZARTH,[1] AND THEO W. DREHER[1,2]*

Department of Agricultural Chemistry[1] and Center for Gene Research and Biotechnology,[2] Oregon State University, Corvallis, Oregon 97331-7301

Received 26 October 1995/Accepted 18 December 1995

The tRNA-like structure (TLS) at the 3′ end of the turnip yellow mosaic virus genome was replaced with heterologous tRNA-like elements, and with a poly(A) tail, in order to assess its role. Replacement with the valylatable TLSs from two closely related tymoviruses resulted in infectious viruses. In contrast, no systemic symptoms on plants, and only low viral accumulations in protoplasts, were observed for three chimeric genomes with 3′ sequences known to enhance mRNA stability and translatability. One of these chimeras had a poly(A) tail, and the others had the TLS with associated upstream pseudoknot tracts from the 3′ ends of brome mosaic and tobacco mosaic viruses. The latter two chimeric RNAs were shown to be appropriately folded by demonstrating their aminoacylation in vitro with tyrosine and histidine, respectively. The results show that enhancement of genome stability or gene expression is not the major role of the turnip yellow mosaic virus TLS. The major role is likely to be replicational, dependent on features present in tymoviral TLSs but not in generic tRNA-like structures.

A striking feature of the 6,318-nucleotide, single-stranded RNA genome of turnip yellow mosaic virus (TYMV) is the tRNA-like structure (TLS) at the 3′ end (Fig. 1). Composed of the 3′-terminal 82 nucleotides of the viral genome, the TLS is efficiently and specifically aminoacylated with valine (21, 42). It can be bound in the aminoacylated state by translational elongation factors EF-Tu (29) and EF-1α (30) and is also a substrate for (CTP, ATP):tRNA nucleotidyltransferase, which can repair incomplete 3′-CCA termini (28). As for $tRNA^{Val}$ (50, 53), the specificity of valine charging is controlled by primary identity nucleotides present in the seven-membered anticodon loop, particularly in the anticodon itself (15). The overall tertiary structure of the TYMV TLS is thought to approximate the L conformation characteristic of tRNAs (16), but the 12-bp acceptor arm differs from tRNA in containing a pseudoknot near the 3′-CCA terminus. RNAs from a number of other tymoviruses have valylatable 3′ TLSs with similar structures, although primary sequences vary considerably (57). TLSs of two other amino acid specificities have been reported as constituents of other positive-strand plant RNA viral genomes: the genomic RNAs from brome mosaic bromovirus (BMV), cucumber mosaic cucumovirus, and barley stripe mosaic hordeivirus accept tyrosine, while the genomic RNA from tobacco mosaic tobamovirus (TMV) accepts histidine (23, 24). These TLSs all contain a pseudoknotted acceptor arm, but the overall structures are more complex and differ markedly from that of the TYMV TLS.

Our previous studies on the role of the TYMV TLS and its aminoacylation used mutations in the valine identity elements to demonstrate that the accumulation of viral RNA and coat protein in transfected protoplasts closely parallels valine acceptance (54, 55). A valylatable TLS thus plays a crucial role in TYMV amplification, but neither its specific function nor that of aminoacylation was clear from those studies. Several possible roles for viral TLSs have been indicated. Studies with BMV have shown that the TLS clearly plays a direct role in RNA replication, since it contains the minus-strand promoter elements necessary for directing minus-strand synthesis (13, 37). At least part of the TYMV minus-strand promoter also appears to be located within the TLS (20), although specific promoter elements have not been identified. Other studies with BMV have implicated host (CTP, ATP):tRNA nucleotidyltransferase in maintaining intact 3′-CCA termini in vivo, revealing a telomeric function for the BMV TLS (44). Gallie and colleagues (19, 35) used reporter gene constructs to show that 3′ sequences from TMV RNA could increase the translational expression and stability of heterologous mRNAs, in an effect comparable to that of a poly(A) tail. Most of the effect was due to a tract of consecutive pseudoknots immediately upstream of the TLS, shown in other studies to be essential for virus viability (52), although the TLS was required for full function. Similar effects were observed for BMV RNA, but the TYMV 3′ untranslated region had a much smaller stimulatory effect on reporter gene expression (18). Other roles, such as in directing viral RNA replication to specific membranes within the cell (17), can also be imagined.

In an effort to address the relative importance of the possible roles of the TYMV TLS and its specific valylation, we have analyzed chimeric genomes in which the 3′-terminal region of TYMC (the Corvallis strain of TYMV) (58) was replaced with heterologous sequences. Some chimeras were designed to test whether generic tRNA-like elements could replace the TLS, or whether the TYMV TLS contains specifically required sequences or structural features. Other chimeras tested the significance of the TLS in promoting genome expression or stability. Finally, chimeras containing the BMV and TMV TLSs offered the opportunity to study the effect of altered amino-

* Corresponding author. Phone: (541) 737-1795. Fax: (541) 737-0497. Electronic mail address: drehert@bcc.orst.edu.

† Technical report no. 10862 of the Oregon Agricultural Experiment Station.

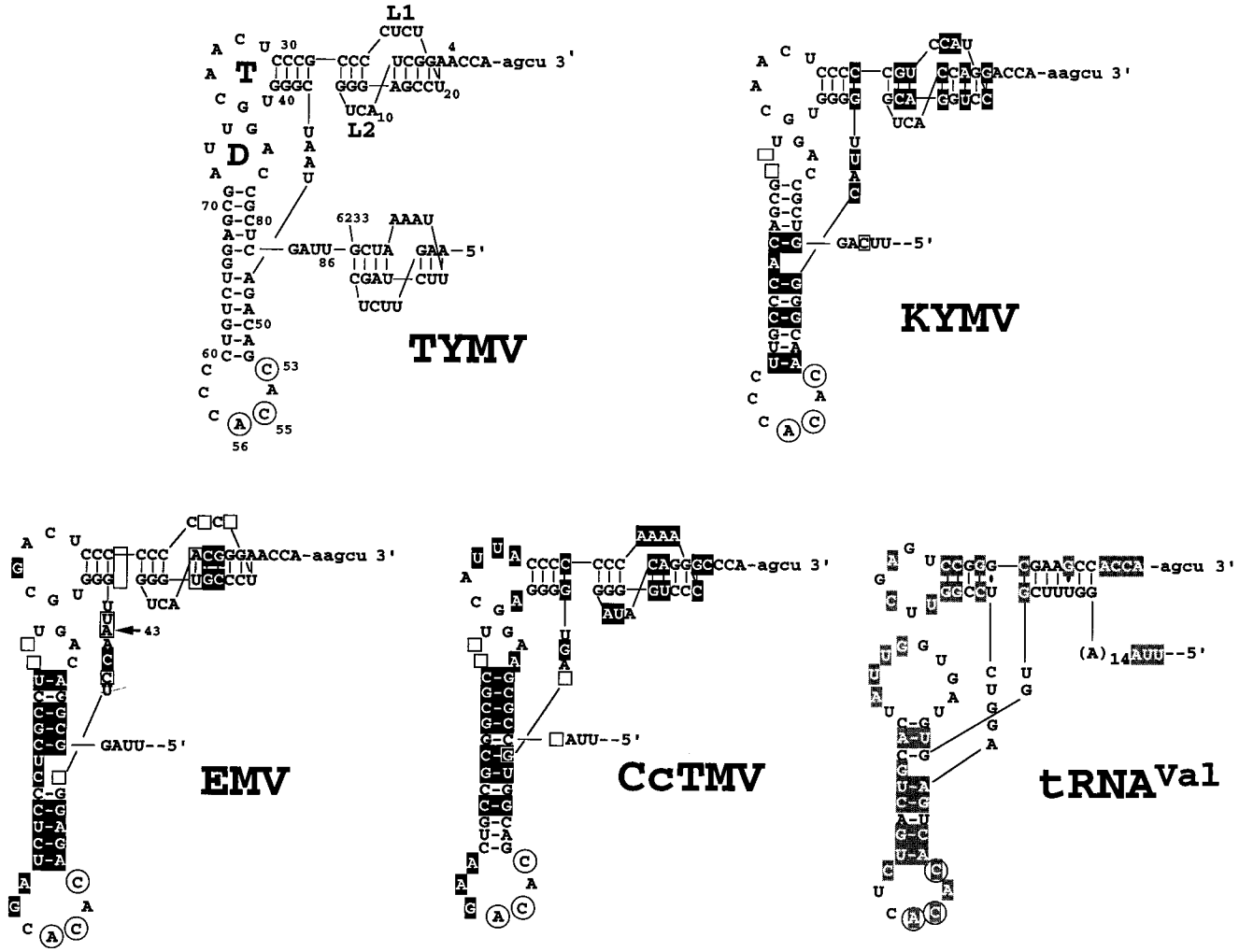

FIG. 1. TLSs present at the 3′ ends of TYMC-derived chimeric genomes. The wild-type TYMV (TYMC) TLS is shown with numbering from the 3′ end. The circled nucleotides represent the primary valine identity elements, and L1 and L2 refer to the loops that bridge helical segments in the acceptor stem pseudoknot. D and T refer to the loops that are analogous to the D and T loops of tRNA. Sequences upstream of the nucleotide marked 6233 (numbering from the 5′ end) are present in all chimeras, and this includes the upstream pseudoknot shown. TLSs from KYMV, EMV, and CcTMV and one based on $tRNA^{Val}$ from lupine (TRVAL) are also shown. The valine identity elements are circled as for TYMV. For the KYMV, EMV, and CcTMV TLSs, inverse shading marks those nucleotides that differ from TYMV RNA; deletions are marked by empty boxes, and insertions are marked by boxed nucleotides. For TRVAL, in view of the different construction with respect to the TYMV TLS, nucleotide identities with TYMV are marked by reverse shading. For the heterologous TLSs, the short string of sequence marked with a 5′ represents the sequence of the connecting string that replaces 86-UUAG in TYMV RNA; these sequences all connect directly to nucleotide 6233, shown in the TYMV structure. For all structures, the nucleotides shown in lower case at the 3′ end are nonviral (vector-derived) nucleotides present on the chimeric transcripts as tested in vivo but not present on transcripts used for in vitro aminoacylation studies. The arrow marking nucleotide 43 of the EMV sequence indicates the presence of an A residue replacing the U present in viral RNA. For TRVAL, the CAC anticodon was used in place of the AAC anticodon in the reported $tRNA^{Val}$ sequence (4).

acylation specificity, albeit in the context of altered sequence and structure. We reasoned that if an interaction between the TLS and a certain host tRNA-associated protein(s) is the primary role of the TLS in transducing its essential function, then various chimeras should replicate to high level. On the other hand, if the TLS plays a more virus-specific role, as is perhaps suggested by the indication that it contains minus-strand promoter elements, then heterologous TLSs would be less likely to work well in chimeric constructs.

MATERIALS AND METHODS

Plant material and virus stocks. Turnip (*Brassica rapa* cv. Just Right) and Chinese cabbage (*B. pekinensis* cv. Spring-A1) were grown in an environmentally controlled chamber at 21°C under 16-h day length. pTYMC is a cDNA-based plasmid clone of TYMC (10) from which infectious RNA can be prepared by in vitro transcription (58). Kennedya yellow mosaic virus-JB (KYMV) and eggplant mosaic virus (EMV) RNAs were provided by A. Gibbs (Australian National University). Plasmid pT7B3Sn (14) was used as a source of the BMV RNA3 3′ noncoding region. CcTMV (the cowpea strain of TMV) and TMV-U1 cDNA clone pTMV104 (8) were gifts from W. O. Dawson (University of Florida).

TYMC and all infectious chimeric viruses were purified from leaves by precipitation with polyethylene glycol according to the procedure of Lane (34). For purification of virion RNAs, virions were disrupted by the addition of 4 to 5 volumes of STE/1 (0.1M Tris-HCl [pH 7.5], 10 mM EDTA, 0.2 M NaCl, and 1% [wt/vol] sodium dodecyl sulfate) and extracted twice with phenol-chloroform (1:1), and the RNA was then precipitated with ethanol in the presence of 2.5 M ammonium acetate.

Construction of chimeric viral genomes. Chimeric sequences (Fig. 1 and 2) were produced by a two-step PCR method involving the initial production of a 3′ megaprimer (48) comprising the non-TYMV part of the chimera fused to TYMC nucleotides corresponding to the sequence immediately upstream of the TYMC TLS. The templates used in producing the megaprimer either were existing cDNA clones (for BMV, BMVPSK, TMV, and TMVPSK chimeras) or were made by reverse transcription-PCR from virion RNA (for KYMV, EMV, and CcTMV chimeras) or by filling out two overlapping synthetic oligonucleotides (for the TRVAL chimera). The 5′ primer contained the junction sequence

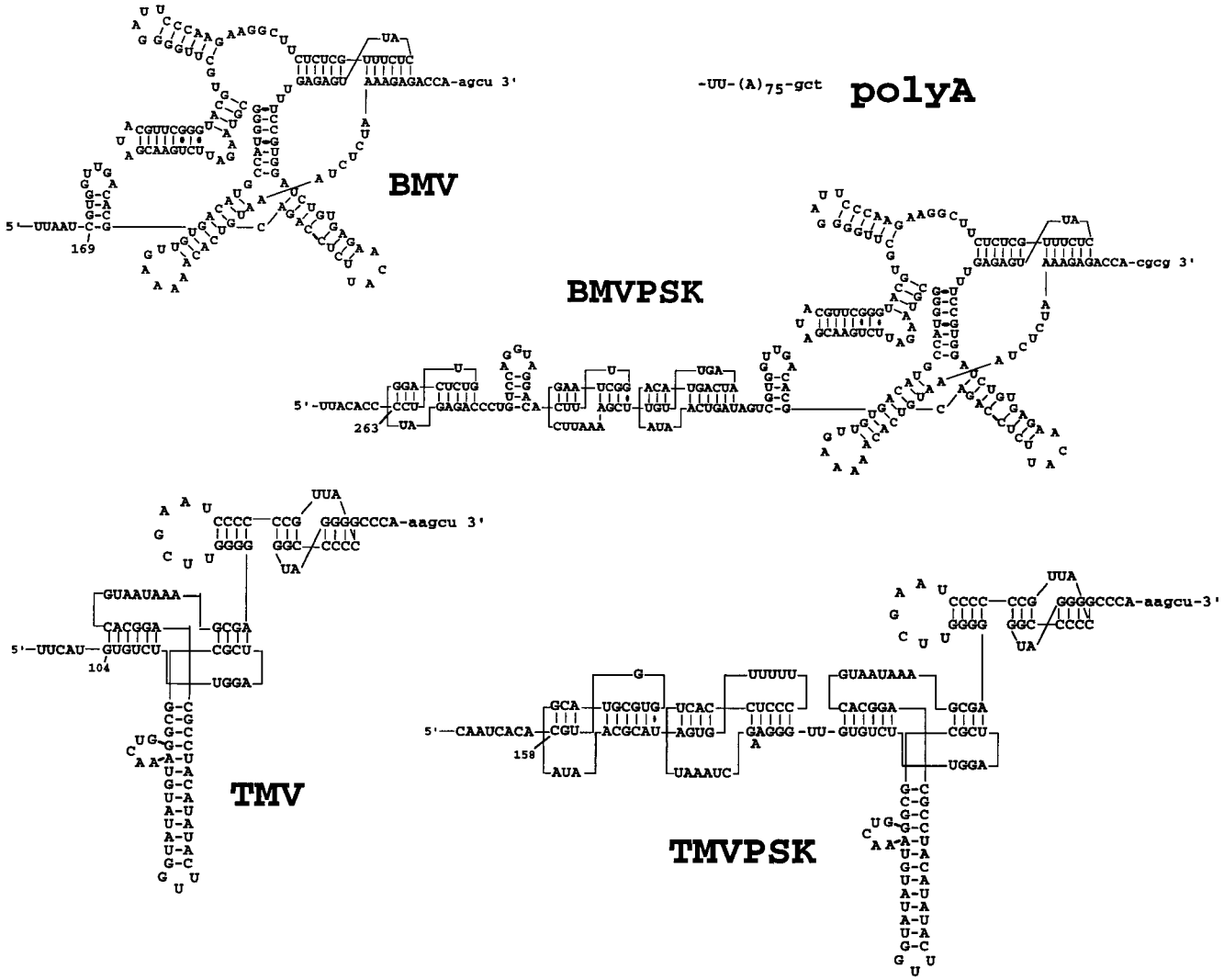

FIG. 2. Nonvalylatable heterologous 3′ sequences present in chimeric genomes. BMV, BMVPSK, TMV, TMVPSK, and polyA represent the heterologous sequences present in the corresponding TYMC-derived chimeric genomes. Conventions regarding sequences at the 5′ and 3′ ends are as in Fig. 1.

for making the chimera, including a short TYMC sequence upstream of nucleotide 6233, while the 3′ primer provided the unique 3′ restriction site used for linearizing transcriptional templates (*Hin*dIII in all cases except BMVPSK, for which *Mlu*I was used because of an internal *Hin*dIII site). The second PCR stage used linearized pTYMC as the template, the megaprimer as the 3′ primer, and a 5′ primer priming at TYMC nucleotide 6014. PCR products were cloned into *Sma*I-cut pUC18, and the sequence of each chimera was verified before subcloning of the *Sma*I (6062)-to-3′-end segment into *Sma*I-*Hin*dIII-cut pTYMC (58). The TYMC-polyA chimera was made by single-step PCR, using the above 5′ primer and a 104-nucleotide-long synthetic oligonucleotide as 3′ primer. Figures 1 and 2 show the chimeric constructs. Note that a mutation (U-43 to A) presumably obtained during PCR is present in the TYMC-EMV chimera (Fig. 1).

In vitro transcription and inoculation of protoplasts and plants. Prior to transcription, plasmids containing wild-type and chimeric viral genomic cDNAs were linearized by digestion with *Hin*dIII (*Mlu*I for pTYMC-BMVPSK). Transcription of 5′-capped genomic RNAs was performed as described previously (58). The concentration and quality of the transcripts were assessed by electrophoresis on nondenaturing 1% agarose gels.

Protoplasts (4×10^5) released from turnip leaves were inoculated with 5 μg of transcript RNAs (59) and incubated for 40 h under constant illumination. At least three independent transcription products corresponding to each viral construct were assayed in at least two independent experiments with separately prepared protoplasts in order to obtain average accumulation data.

Three- to four-week-old Chinese cabbage plants were inoculated with either lysates of infected protoplasts (59) or genomic transcripts (2.5 μg) in 50 μl of 50 mM glycine–30 mM K_2HPO_4 (pH 9.2)–1% (wt/vol) Celite–3 mg of bentonite per ml. Virions were passaged by inoculating seedlings with purified virions (5 μg) in 50 μl of 0.1 M potassium phosphate (pH 7.0)–1% (wt/vol) Celite.

Analysis of viral products. Total cellular RNA was isolated from protoplasts, glyoxalated, and subjected to Northern (RNA) blot analysis as described previously (58). In the present study, the hybridization probe consisted of a minus-sense in vitro transcript complementary to nucleotides 5708 to 5988 in the coat protein coding region of the TYMV genome. Levels of viral RNA were quantified by analysis of hybridization signals in a PhosphorImager (Molecular Dynamics, Inc.), with reference to a dilution series of viral RNA standards on the same blot. Coat protein accumulation was monitored by Western blot (immunoblot) analysis as described (58) except that detection was by enhanced chemiluminescence (ECL kit; Amersham).

To analyze progeny virion RNA sequences, virion RNAs were polyadenylated by using bacterial poly(A) polymerase (Gibco-BRL), and DNA corresponding to the 3′-terminal 264 nucleotides of TYMC (or infectious chimeras) was prepared by reverse transcription-PCR. The deoxyoligonucleotide $(T)_{35}GG$ was used as the primer for reverse transcription, and as the 3′ primer in PCR amplifications, to permit sequence analysis of all nucleotides upstream of the 3′-CCA. The PCR products were sequenced by using a cycle sequencing protocol in an air thermocycler (51), with a 5′-^{32}P-end-labeled primer corresponding to TYMV RNA nucleotides 6139 to 6156.

Aminoacylation studies. Chimeric RNAs for aminoacylation analyses were prepared by in vitro transcription using T7 RNA polymerase and PCR-generated templates as described previously (56). RNAs were incubated at a concentration of either 0.1 or 0.2 μM at 30°C with aminoacyl-tRNA synthetase activities that

TABLE 1. Replication of TYMC-derived chimeric RNAs in turnip protoplasts and Chinese cabbage plants

RNA	Relative amplification in protoplasts[a]	Systemic infection in plants[b]		
		No. symptomatic/no. inoculated	No. of days to symptoms	Virion yield (mg/g [fresh wt])
TYMC	1.0	6/6	7–8	1.89
TYMC-KYMV	0.36	3/3	10	1.24
TYMC-EMV	0.22	2/5	16–31	0.16
TYMC-CcTMV	NDS	—	—	—
TYMC-TRVAL	NDS	—	—	—
TYMC-BMV	0.002	0/3	—	—
TYMC-BMVPSK	0.01	0/4	—	—
TYMC-TMV	NDS	0/10	—	—
TYMC-TMVPSK	0.035	0/10	—	—
TYMC-polyA	NDS	0/2	—	—

[a] Relative levels of genomic RNA detected in extracts made from turnip protoplasts 40 h postinoculation, determined by Northern blotting as shown in Fig. 3 and 5. NDS, no detectable signal, i.e., ≤0.001 relative to TYMC. TYMC is the cloned genotype of TYMV used in these studies.

[b] Analysis of infectivity in Chinese cabbage plants. Most inoculations were with RNA transcripts, although some were with lysates of infected protoplasts. —, no experiment performed.

were partially purified from wheat germ (15) and used at 0.13 μg of protein per ml. The buffers used for valylation assays were the standard valylation buffer TM (25 mM Tris-HCl [pH 8.0], 2 mM $MgCl_2$, 0.1 mM spermine, 1 mM ATP) (15) and IV (30 mM *N*-2-hydroxyethylpiperazine-*N*′-2-ethanesulfonic acid [HEPES]-KOH [pH 7.5], 100 mM potassium acetate, 2.5 mM magnesium acetate, 1.5 mM ATP), which more closely mimics in vivo conditions. For tyrosylation assays, we used IV and HAM (0.1 M HEPES-KOH [pH 7.5], 48 mM KCl, 5 mM $MgCl_2$, 0.64 mM ATP) (11). Histidylation assays were carried out with three buffers: TM, IV, and HY (25 mM Tris-HCl [pH 8.5], 7.5 mM $MgCl_2$, 0.5 mM ATP), the latter corresponding to conditions used with yeast HisRS histidyl-tRNA synthetase (47). In all cases, the appropriate ^{3}H-labeled amino acid was present at 10 μM. Assays were conducted as previously described (15).

RESULTS

Design of chimeric genomes. The successful application of a strategy involving the transplantation of heterologous RNA structural elements relies on constructing the chimera in a way that does not disrupt the folding of those elements. In considering the precise sequence at the splice site of the chimeras, we used the RNA folding algorithm STAR (1) to help avoid designing chimeric RNAs with stable, undesired conformations. All chimeras contain TYMC nucleotides 1 to 6233, thus including the pseudoknot immediately upstream of the TLS that appears to be required for full viral function (55). In TYMC RNA, the sequence 5′ -UUAG- connects to the 82-nucleotide-long TLS (Fig. 1). The corresponding connecting sequence varies slightly in the different chimeras (Fig. 1 and 2), as a result of selecting sequences likely to avoid alternative, unwanted conformations. Aminoacylation activity, discussed below, is a functional assay that requires a properly folded TLS and so provides a measure of the degree to which the expected conformations are present for each chimera.

Infectivity of chimeric viruses possessing valine identity elements. Since previous studies demonstrated that efficient TYMV RNA amplification in cells required the presence in the TLS of intact valine identity elements (54), it was of interest to test whether other TLSs with valine identity were able to functionally substitute for the TYMV TLS in an in vivo replication assay. Four chimeras with heterologous valylatable TLSs were constructed (Fig. 1). Two chimeras, TYMC-KYMV and TYMC-EMV, contain TLSs from the tymoviruses KYMV (9) and EMV (39), respectively. Chimera TYMC-CcTMV contains the TLS from the CcTMV (also called Sunnhemp mosaic virus) (36). All three TLSs are structurally very similar to the TYMV TLS, although there are numerous differences in primary sequence. Chimera TYMC-TRVAL contains the 76-nucleotide sequence of lupine $tRNA^{Val}$ (4) connected to the remainder of the genome via an $UU(A)_{15}$ spacer. Note that unlike the other three constructs, the TRVAL TLS is connected to the genome from a point close to the 3′-CCA terminus. All constructs contain the strong valine identity elements in the anticodon loop that were shown to be essential for valylation by wheat germ valyl-tRNA synthetase (ValRS) (15) (circled in Fig. 1).

Turnip protoplasts were transfected with wild-type and chimeric genomic transcripts (5′ capped), and the accumulations of viral products were analyzed 40 h postinoculation. Plants (Chinese cabbage) were also inoculated. Only TYMC-KYMV and TYMC-EMV chimeras were able to establish systemic infection in plants (Table 1). Infectivity was high for TYMC-KYMV, with all inoculated plants exhibiting symptoms with only a 2- to 3-day delay relative to the wild type and with high levels of virus produced. TYMC-EMV was less infectious, producing symptoms in less than half of the inoculated plants after an 8- to 23-day delay and accumulating to about 1/10 of the levels of wild-type TYMC (Table 1). Nevertheless, the production of infectious virus in plants indicates a high level of fitness. The delayed appearance of symptoms after inoculation with TYMC-EMV was retained in subsequent passages using purified virion inocula, suggesting that the delayed symptom appearance was not the result of selection of a genetic variant. Direct sequence analysis of the 3′-terminal ca. 160 nucleotides of progeny virion RNA (second passage for TYMC-KYMV and sixth passage for TYMC-EMV) showed no sequence changes (data not shown), confirming the replication of the chimeric sequences shown in Fig. 1.

TYMC-KYMV and TYMC-EMV also amplified fairly efficiently in turnip protoplasts, as evidenced by Northern blots detecting viral genomic and subgenomic RNAs (Fig. 3) and Western blots detecting coat protein (not shown). As in the plants, TYMC-KYMV amplified to higher levels than TYMC-EMV (0.36 and 0.22 relative to TYMC, respectively, on the basis of Northern blots; Table 1).

Neither TYMC-CcTMV nor TYMC-TRVAL amplified to produce detectable levels in Northern (Fig. 3) or Western (not shown) blot assays of inoculated protoplasts, indicating accumulation below the detection limit of ca. 0.001 to 0.005 relative

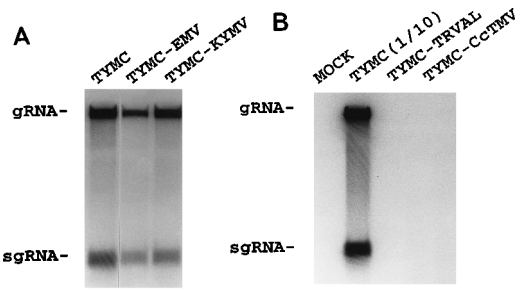

FIG. 3. Amplification in turnip protoplasts of chimeric genomes with valine identity elements. Northern blot analysis was performed after separation on 1% agarose of extracts from protoplasts inoculated with capped genomic transcript RNAs and harvested 40 h postinoculation. Progeny genomic RNA (gRNA) and subgenomic RNA (sgRNA) were detected by hybridization with a riboprobe complementary to a portion of the coat protein coding region that is present in all constructs. Extracts representing 27,000 (A) and 74,000 (B) protoplasts were loaded on lanes [except that 7,400 protoplasts were loaded for lane TYMC(1/10)].

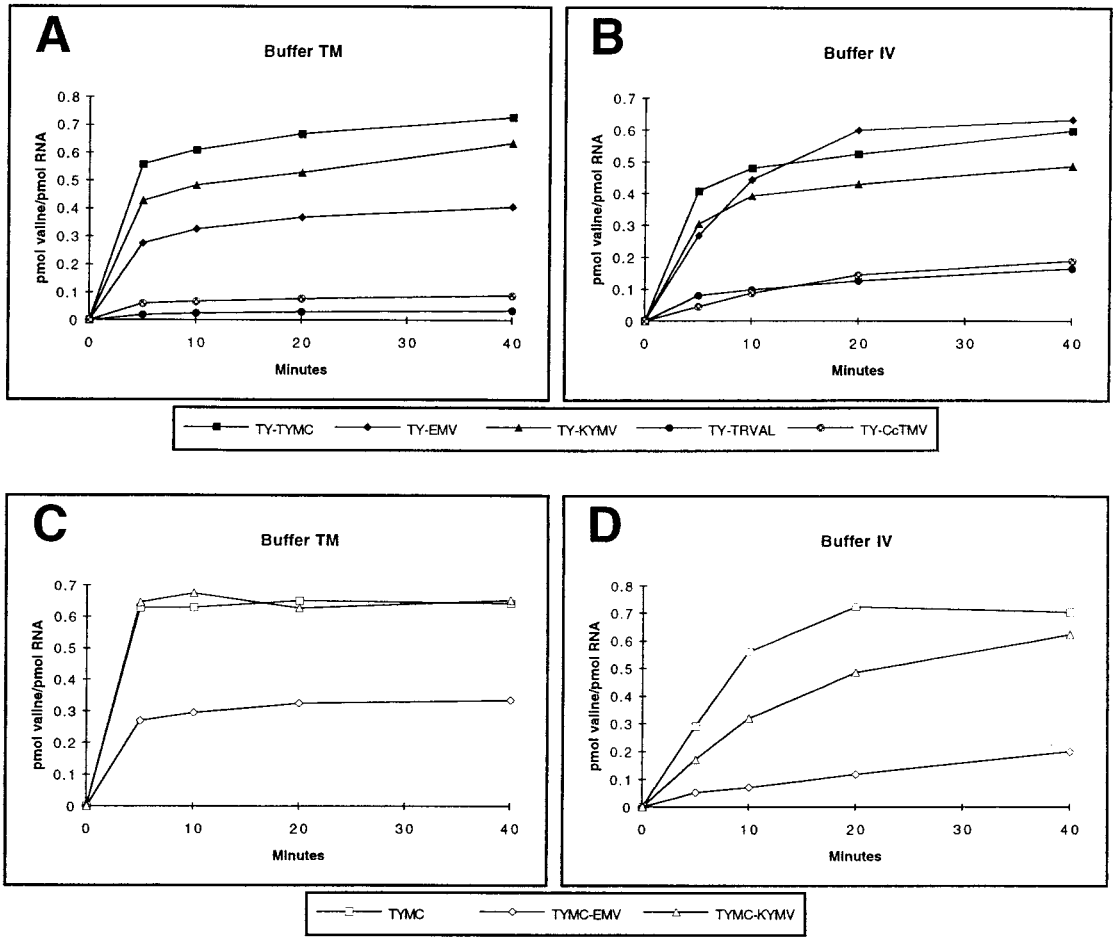

FIG. 4. Valylation by wheat germ valyl-tRNA synthetase of chimeric RNAs with valine identity elements. Aminoacylation reactions were conducted at 0.2 μM RNA in the buffer conditions indicated. (A and B) In vitro transcripts derived from the 264-nucleotide-long wild-type TY-Sma RNA; (C and D) progeny virion RNAs isolated from infected plants. In each case, the RNAs are identified by the legends below the graphs. The presented results are averages of two experiments.

to TYMC (depending on the experiment). Likewise, no virus infections were observed on inoculated plants.

The in vitro valylation by wheat germ ValRS of chimeric RNAs was studied. Two buffers were used: TM, a low-ionic-strength buffer used previously (15), and IV, a buffer that approximates the conditions in a typical in vitro translation reaction and is meant to better represent in vivo conditions. Transcripts corresponding to the 3′-terminal 264 nucleotides of TYMC RNA (TY-TYMC; TY-Sma in reference 12), which terminated in the correct 3′-CCA, were studied for all four chimeras (these are referred to as TY-KYMV, etc.) (Fig. 4A and B). In addition, the valylation of progeny virion RNAs was studied for TYMC, TYMC-KYMV, and TYMC-EMV (Fig. 4C and D). TY-TYMC RNA and virion TYMC RNA became 60 to 70% valylated in both buffer conditions. TY-KYMV and virion TYMC-KYMV RNAs also became valylated to about the same level, although charging was slower in IV buffer. TY-EMV and the corresponding virion RNA both became 30 to 40% valylated in TM buffer. In IV buffer, TY-EMV RNA accepted valine as efficiently as TY-TYMC, but the virion TYMC-EMV RNA became valylated slowly, without reaching plateau by 40 min. These results show that both the KYMV and EMV chimeric RNAs can be substantially valylated, indicating the correct folding of these TLSs in their new (TYMC) context. The reason for the low valine acceptance of virion TYMC-EMV RNA in the IV conditions is uncertain, but if this result does indeed reflect the situation in vivo, then the less efficient valylation may be a factor contributing to the decreased accumulation in protoplasts and plants compared with TYMC-KYMV. Recall that the valine acceptance of TYMV RNA is an important determinant of in vivo accumulation levels (54). Previous studies reported 35 to 40% valylation of EMV RNA by wheat germ ValRS (41).

TY-CcTMV and TY-TRVAL RNAs became valylated to levels well below that for TY-TYMC in both buffers (Fig. 4A and B). In IV buffer, the valylation levels of both RNAs were similar to that of virion TYMC-EMV (i.e., 15 to 20%). Valylation levels were lower in TM buffer, 9% for TY-CcTMV and 4% for TY-TRVAL. These results suggest that the majority of molecules of these two chimeras have not folded properly or that these RNAs do not have high valine acceptance despite the presence of the major valine identity elements in the anticodon loop (Fig. 1). Indeed, Beachy et al. (6) report valylation levels of 6 to 21% for different preparations of CcTMV RNA, as catalyzed by a yeast ValRS activity in 0.1 M Tris-HCl (pH 7.4)–20 mM $MgCl_2$–2 mM mercaptoethanol. The CcTMV TLS may thus contain some features that act as antideterminants toward ValRS and prevent full valylation, and the TLS in the chimera may not in fact be malfolded. As for TY-CcTMV RNA, the poor valylation of TY-TRVAL RNA may be due to

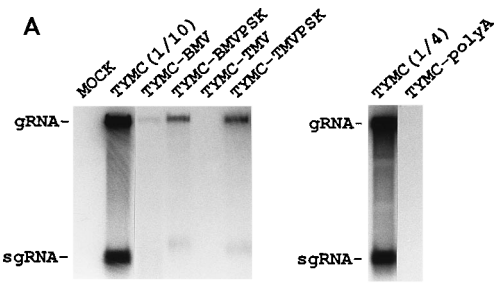

FIG. 5. Amplification in turnip protoplasts of chimeric genomes without valine identity elements. Extracts were made from protoplasts 40 h after inoculation with the indicated RNAs, and progeny viral RNAs were detected in Northern blots as in Fig. 3. Subgenomic RNAs were not underrepresented in other experiments. (A) Extracts representing 74,000 protoplasts were loaded on lanes [except that 7,400 protoplasts were loaded for lane TYMC(1/10)]. (B) Extracts from 10,000 protoplasts were loaded in lane TYMC(1/4), and extracts from 40,000 protoplasts were loaded in lane TYMC-polyA. gRNA and sgRNA, genomic and subgenomic RNAs.

improper folding or an intrinsically low valine acceptance. The latter may be caused by the mode of attachment to the remainder of the genome, since $tRNA^{Val}$ transcripts were efficiently valylated (not shown). Short 5′ extensions of at least some tRNAs do not interfere with aminoacylation (e.g., reference 40), although this is likely to be strongly sequence-dependent.

Infectivity of chimeric viruses with histidine- and tyrosine-charging TLSs and with a poly(A) tail. BMV and TMV RNAs possess TLSs that can be tyrosylated (25) and histidylated (38), respectively. In both viral RNAs, there is a tract of at least three consecutive pseudoknots immediately upstream of the TLS (43). For BMV (33) and TMV (52), viral RNA amplification levels were seriously decreased when part or all of this tract was deleted. Studies by Gallie and coworkers have implicated these regions of the viral genomes in promoting gene expression and stability (18, 19). We made two types of chimeras with sequences from BMV RNA3 (2) and TMV-U1 (same as vulgare strain) (22) (Fig. 2), those carrying the heterologous TLS alone (TYMC-BMV and TYMC-TMV), and those that in addition carry the upstream pseudoknot tract (TYMC-BMVPSK and TYMC-TMVPSK). The PSK-containing chimeras were thought more likely to present the TLS in a correctly folded form, and in a state accessible to enzymes (e.g., aminoacyl-tRNA synthetase), but were also designed as a test of the role of viral 3′ ends in enhancing genome expression and stability. This latter point was further addressed with chimera TYMC-polyA (Fig. 2), in which the TYMV TLS was replaced with a 75-residue long poly(A) tail.

Chimera TYMC-BMV amplified to very low levels in turnip protoplasts (ca. 0.2% relative to TYMC), while TYMC-TMV failed to accumulate to detectable levels (Fig. 5 and Table 1). However, when the constructs also included the upstream pseudoknots, viral accumulation was increased to 1 and 3% relative to TYMC for TYMC-BMVPSK and TYMC-TMVPSK, respectively (Fig. 5 and Table 1). TYMC-polyA failed to accumulate to detectable levels in turnip protoplasts. None of these five constructs elicited systemic symptoms in Chinese cabbage plants or produced asymptomatic infections (in those plants checked). In the past, we have been successful in isolating informative second-site suppressor mutations after inoculating poorly replicating genomes onto plants and waiting for late-onset symptoms (55). For TYMC-TMVPSK, which replicated to the highest levels within this group of chimeras, the plasmid was passaged up to three times through mutator strains of *Escherichia coli* (*mutD5* strain NR9232 [49] or XL1-Red [Stratagene, Inc.]) before transcription, in an effort to introduce genetic changes that might increase the infectivity in plants. No symptomatic plants appeared, however, suggesting that the types or extents of sequence changes that can be introduced in the mutator strains or by replication errors in planta are not sufficient to improve the fitness of TYMC-TMVPSK to a level that results in systemic infection in plants.

The tyrosylation of TY-BMV and TY-BMVPSK RNAs was studied with wheat germ tyrosyl-tRNA synthetase, in IV and HAM (11) buffers. (The use of TM buffer resulted in low tyrosylation rates.) The tyrosylation efficiency of TY-BMVPSK was close to that of the control virion BMV RNA in HAM buffer, with 90 to 100% of molecules becoming charged, while TY-BMV RNA became 63% charged after 40 min (Fig. 6). Tyrosylation rates of all three RNAs were slower in IV buffer, and differences between the RNAs were more pronounced: virion BMV, TY-BMVPSK, and TY-BMV RNAs became 90, 38, and 6% tyrosylated, respectively.

The levels of histidylation of TY-TMV and TY-TMVPSK RNAs were also studied with wheat germ histidyl-tRNA synthetase, in IV, TM and HY buffers. TM and HY conditions gave equivalent results, and only the TM buffer results are given. Although $tRNA^{His}$ could be fully charged in TM buffer, and nearly so in IV buffer, the histidine acceptance of both TMV-derived RNAs was lower: TY-TMVPSK and TY-TMV RNAs became 59 and 25% histidylated, respectively, in TM buffer (Fig. 7). In IV buffer, the histidylation of the TMV-

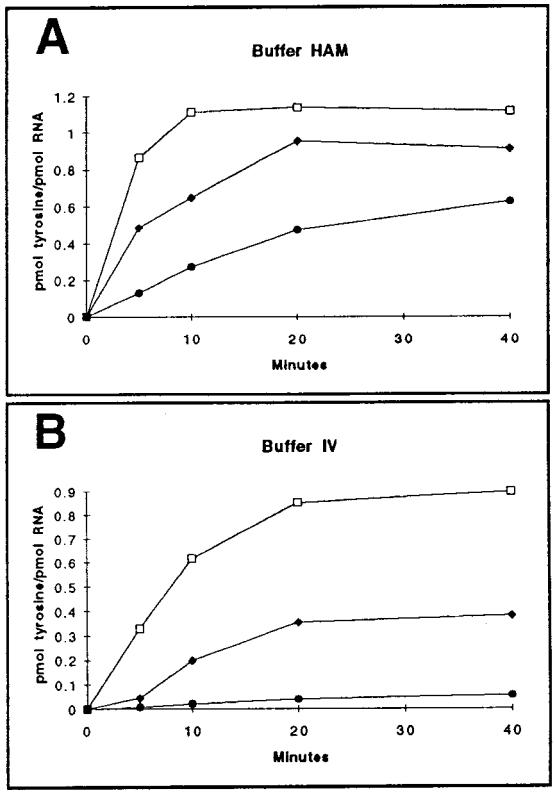

FIG. 6. Tyrosylation by wheat germ tyrosyl-tRNA synthetase of chimeric RNAs derived from BMV RNA. Aminoacylation reactions were conducted at 0.2 μM RNA in the buffer conditions indicated. The levels of tyrosylation of TY-BMV (●) and TY-BMVPSK (◆) in vitro transcripts are compared with that of BMV virion RNA (□). The presented results are averages of two experiments. Aminoacylation above 1.0 is due to error in estimating the concentration of 3′ termini.

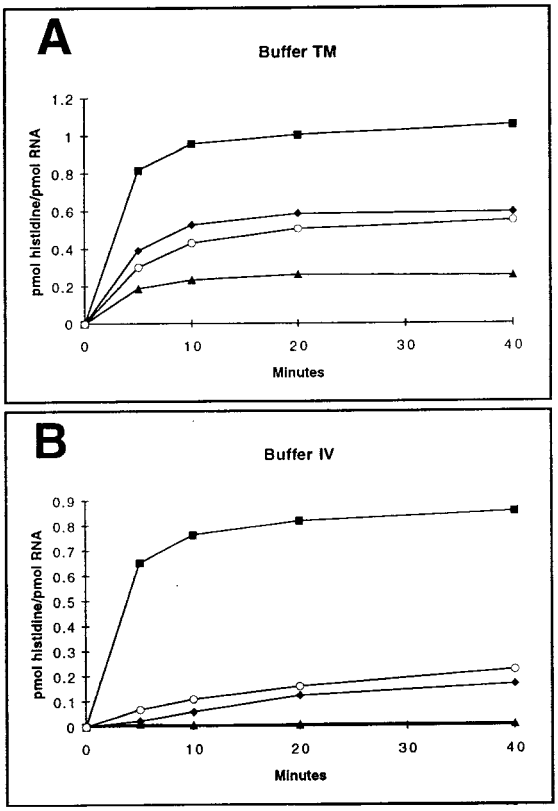

FIG. 7. Histidylation by wheat germ histidyl-tRNA synthetase of chimeric RNAs derived from TMV RNA. Aminoacylation reactions were conducted at 0.2 μM RNA in the buffer conditions indicated. The levels of histidylation of TY-TMV (▲) and TY-TMVPSK (◆) in vitro transcripts are compared with that of an in vitro transcript of lupine $tRNA^{His}$ (5) made from a synthetic gene (■) and with that of TMV virion RNA (○). The presented results are averages of two experiments.

derivedRNAs was lower (17% for TY-TMVPSK), and it was barely detectable for TY-TMV RNA (0.8%). In parallel with these experiments, we observed that TY-CcTMV RNA does not detectably accept histidine (not shown), confirming this TLS as being valine specific (6).

The aminoacylation properties of the chimeras containing BMV and TMV RNA sequences are clearly improved by the presence of the upstream pseudoknot domain, paralleling the higher in vivo accumulation rates when the upstream pseudoknots were present. TY-TMV and TY-BMV RNAs were poorly aminoacylated under IV buffer conditions, suggesting that the TLSs in these constructs were improperly folded (note, however, that the higher aminoacylation in TM buffer shows that proper folding can occur under some conditions). The aminoacylation levels of TY-BMVPSK and TY-TMVPSK RNAs indicate that the TLSs of these constructs are substantially correctly folded. The aminoacylation levels of TY-TMVPSK reflect the range of histidylation reported in the literature for TMV RNA (6, 7, 31, 38).

DISCUSSION

The TYMV TLS cannot be functionally replaced by generic tRNA-like structures, and its major role is not to enhance genome expression and stability. Our experiments have answered the fundamental question as to whether the TYMV TLS functions as a generic tRNA-like element capable of directing aminoacylation, or whether its function is virus specific. A priori, either scenario seemed possible. On the one hand, positive-strand RNA plant viruses closely related on the basis of the phylogeny of their essential helicase-like and polymerase-like proteins may have very different features at the 3′ ends of their genomes. Thus, the carla- and potexviruses, which are the closest relatives of the tymoviruses (9, 32), have polyadenylated genomes. In view of the functional similarity between a poly(A) tail and at least some plant viral 3′ untranslated regions in stabilizing mRNAs and increasing translational expression (18, 19), one might expect the TYMV TLS to serve in these roles. Since this would be through interactions with host rather than viral proteins, the TLS would act as a generic tRNA mimic. On the other hand, the TLS of BMV RNA contains the minus-strand promoter (13, 37), and there is some indication that this is also true of the TYMV TLS (20). This would suggest the presence of virus-specific features in the TLS that are superimposed on the tRNA mimicry. Indeed, replacement of the TMV RNA 3′ region with BMV 3′ sequences resulted in very low amplification (0.001 to 0.01 relative to the wild type) (26).

The chimeric genomes that we have studied replaced the TYMV TLS with diverse tRNA-like elements. Only replacement with TLSs from other tymoviruses (KYMV and EMV) resulted in viruses that replicated efficiently in protoplasts (Fig. 3) and produced systemic symptoms in plants (Table 1). Chimeras TYMC-BMVPSK and TYMC-TMVPSK, which had functional TLSs on the basis of their aminoacylation properties, accumulated in protoplasts to levels below 4% of that for wild-type TYMC (Fig. 5 and Table 1). Clearly, these heterologous TLSs are not able to functionally replace the TYMV TLS. The failure of these chimeras to amplify should not be due to any defect in viral gene expression or due to a shorter genomic RNA half-life, since the 3′ sequences from both TMV and BMV are known to enhance these properties (18). Rather, the chimeras most likely have a replication defect that could result from the lack of specific minus strand promoter.

The failure of TYMC-BMVPSK and TYMC-TMVPSK RNAs, along with TYMC-polyA RNA, to replicate above very low levels shows emphatically that enhancing genome stability and translational expression is not the major role of the TYMV TLS. This conclusion is in line with the findings (18) that the TYMV RNA 3′ untranslated region provided only a 4-fold enhancement of reporter gene expression, compared with 30- to 50-fold for the 3′ sequences from BMV and TMV RNA, and similar results for a poly(A) tail (19). While replicational functions are likely to be the major role of the TYMV TLS, as has been concluded for the BMV 3′ region (33), secondary roles in genome stabilization and expression (consider also reference 44) are probably of some importance. It is interesting that TYMC-BMVPSK and TYMC-TMVPSK accumulated to detectable levels, while TYMC-polyA did not. Apparently the viral 3′ regions are more acceptable to the TYMV replicational machinery, perhaps reflecting a common evolutionary origin for plant viral TLSs.

The TYMV TLS can be functionally replaced by TLSs from other tymoviruses. TYMC-KYMV and TYMC-EMV are highly viable chimeras (Table 1). This is perhaps not surprising, since compatibility between the replicational machinery and 3′ RNA termini has been observed previously between viruses from the same group. Thus, RNA3 components can be switched between cucumber mosaic and tomato aspermy cucumoviruses (45), and between the bromoviruses BMV and cowpea chlorotic mottle viruses (3), to make viable pseudorecombinant viruses. Viable chimeras with 3′ switches similar to those reported in this paper have also been constructed

between tobamoviruses (27), and even between BMV and cucumber mosaic virus (46), which are from two different groups but have TLSs that are at least as similar in sequence and structure (2) as the tymoviral TLSs that we have studied.

These observations all lead to the conclusion that TLS functions are well conserved between closely related viruses. Nevertheless, it is interesting that in replacing the TYMV TLS with that of KYMV and EMV, most of the nucleotides in the TLS have been substituted (Fig. 1). Analysis of the sequences common to the three TLSs should provide candidate minus-strand promoter elements, bearing in mind that the poorer amplification of TYMC-EMV than of TYMC-KYMV may reflect the loss of some promoter function. The sequences of the D and T loops at the corner of the L conformation are conserved, but their function is probably in maintaining the tRNA-like conformation. The identity elements in the anticodon loop are also conserved, but we have recently shown, by constructing a viable virus in which these nucleotides were changed to confer methionylation (15a), that these valine identity elements are not inviolate. The most likely common elements for specific recognition are loops L1 and L2 in the acceptor stem pseudoknot and perhaps sequences in the single-stranded connection between the two halves of the L (Fig. 1). These features differ quite markedly in sequence for the CcTMV TLS and are absent in the TYMC-TRVAL chimera (Fig. 1); this may be an important reason for the failure of these chimeras to replicate detectably, although this may also be due to their poor aminoacylation or inappropriate folding. The different distribution of base pairs among the three helical segments of the acceptor stem of the EMV TLS (6:3:3 rather than 5:3:4 as in TYMV and KYMV; Fig. 1) may play a role in the somewhat lower amplification of the TYMC-EMV chimera (Table 1).

ACKNOWLEDGMENTS

We thank W. O. Dawson and A. Gibbs for supplying plasmids and viral RNAs and R. Schaaper for supplying *E. coli* NR9232. We thank Kirsten Wolthers for help in experiments with *E. coli* mutator strains.

This study was supported by NSF grant DMB-9019174.

REFERENCES

1. **Abrahams, J. P., M. van den Berg, E. van Batenburg, and C. Pleij.** 1990. Prediction of RNA secondary structure, including pseudoknotting, by computer simulation. Nucleic Acids Res. **18:**3035–3044.
2. **Ahlquist, P., R. Dasgupta, and P. Kaesberg.** 1981. Near identity of 3′ RNA secondary structure in bromoviruses and cucumber mosaic virus. Cell **23:** 183–189.
3. **Allison, R. F., M. Janda, and P. Ahlquist.** 1988. Infectious in vitro transcripts from cowpea chlorotic mottle virus cDNA clones and exchange of individual RNA components with brome mosaic virus. J. Virol. **62:**3581–3588.
4. **Barciszewska, M., and D. S. Jones.** The nucleotide sequence of a valine accepting tRNA from *Lupinus luteus* (lupin) seeds. Nucleic Acids Res. **15:** 1333.
5. **Barciszewska, M. Z., G. Keith, G. Dirheimer, and J. Barciszewski.** 1986. The primary structure of the first plant $tRNA^{His}$. Plant Sci. **47:**103–107.
6. **Beachy, R. N., M. Zaitlin, G. Bruening, and H. W. Israel.** 1976. A genetic map for the cowpea strain of TMV. Virology **73:**498–507.
7. **Carriquiry, E., and S. Litvak.** 1974. Further studies on the enzymatic aminoacylation of tobacco mosaic virus RNA by histidine. FEBS Lett. **38:**287–291.
8. **Dawson, W. O., D. L. Beck, D. A. Knorr, and G. L. Grantham.** 1986. cDNA cloning of the complete genome of tobacco mosaic virus and production of infectious transcripts. Proc. Natl. Acad. Sci. USA **83:**1832–1836.
9. **Ding, S., P. Keese, and A. Gibbs.** 1990. The nucleotide sequence of the genomic RNA of kennedya yellow mosaic tymovirus-Jervis Bay isolate: relationships with potex- and carlaviruses. J. Gen. Virol. **71:**925–931.
10. **Dreher, T. W., and K. L. Bransom.** 1992. Genomic RNA sequence of turnip yellow mosaic virus isolate TYMC, a cDNA-based clone with verified infectivity. Plant Mol. Biol. **18:**403–406.
11. **Dreher, T. W., J. J. Bujarski, and T. C. Hall.** 1984. Mutant viral RNAs synthesized *in vitro* show altered aminoacylation and replicase template activities. Nature (London) **311:**171–175.
12. **Dreher, T. W., C. Florentz, and R. Giegé.** 1988. Valylation of tRNA-like transcripts from cloned cDNA of turnip yellow mosaic virus RNA demonstrates that the L-shaped region at the 3′ end of the viral RNA is not sufficient for optimal aminoacylation. Biochimie **70:**1719–1727.
13. **Dreher, T. W., and T. C. Hall.** 1988. Mutational analysis of the sequence and structural requirements in brome mosaic virus RNA for (−) strand promoter activity. J. Mol. Biol. **201:**31–40.
14. **Dreher, T. W., A. L. N. Rao, and T. C. Hall.** 1989. Replication *in vivo* of mutant brome mosaic virus RNAs defective in aminoacylation. J. Mol. Biol. **206:**425–438.
15. **Dreher, T. W., C.-H. Tsai, C. Florentz, and R. Giegé.** 1992. Specific valylation of turnip yellow mosaic virus RNA by wheat germ valyl-tRNA synthetase is determined by three anticodon loop nucleotides. Biochemistry **31:**9183–9189.

15a. **Dreher, T. W., C.-H. Tsai, and J. M. Skuzeski.** Submitted for publication.

16. **Dumas, P., D. Moras, C. Florentz, R. Giegé, P. Verlaan, A. van Belkum, and C. W. A. Pleij.** 1987. 3-D graphics modeling of the tRNA-like 3′-end of turnip yellow mosaic virus RNA: structural and functional implications. J. Biomol. Struct. Dyn. **4:**707–728.
17. **Francki, R. I. B.** 1987. Responses of plant cells to virus infection with special reference to the sites of RNA replication, p. 423–436. *In* M. A. Brinton and R. R. Rueckert (ed.), Positive strand RNA viruses. Alan R. Liss, Inc., New York.
18. **Gallie, D. R., and M. Kobayashi.** 1994. The role of the 3′ untranslated region of non-polyadenylated plant viral mRNAs in regulating translational efficiency. Gene **142:**159–165.
19. **Gallie, D. R., and V. Walbot.** 1990. RNA pseudoknot domain of tobacco mosaic virus can functionally substitute for a poly(A) tail in plant and animal cells. Genes Dev. **4:**1149–1157.
20. **Gargouri-Bouzid, R., C. David, and A.-L. Haenni.** 1991. The 3′ promoter region involved in RNA synthesis directed by the turnip yellow mosaic virus genome *in vitro*. FEBS Lett. **294:**56–58.
21. **Giegé, R., J. P. Briand, R. Mengual, J. P. Ebel, and L. Hirth.** 1978. Valylation of the two RNA components of turnip yellow mosaic virus and specificity of the tRNA aminoacylation reaction. Eur. J. Biochem. **84:**251–256.
22. **Goelet, P., G. P. Lomonossoff, P. J. G. Butler, M. E. Akam, M. J. Gait, and J. Karn.** 1982. Nucleotide sequence of tobacco mosaic virus RNA. Proc. Natl. Acad. Sci. USA **79:**5818–5822.
23. **Hall, T. C.** 1979. Transfer RNA-like structures in viral genomes. Int. Rev. Cytol. **60:**1–26.
24. **Mans, R. M., C. W. Pleij, and L. Bosch.** 1991. tRNA-like structures: structure, function and evolutionary significance. Eur. J. Biochem. **201:**303–324.
25. **Hall, T. C., D. S. Shih, and P. Kaesberg.** 1972. Enzyme-mediated binding of tyrosine to brome mosaic virus RNA. Biochem. J. **129:**969–976.
26. **Ishikawa, M., P. Kroner, P. Ahlquist, and T. Meshi.** 1991. Biological activities of hybrid RNAs generated by 3′-end exchanges between tobacco mosaic and brome mosaic viruses. J. Virol. **65:**3451–3459.
27. **Ishikawa, M., T. Meshi, Y. Watanabe, and Y. Okada.** 1988. Replication of chimeric tobacco mosaic viruses which carry heterologous combinations of replicase genes and 3′ noncoding regions. Virology **164:**290–293.
28. **Joshi, S., F. Chapeville, and A.-L. Haenni.** 1982. Length requirements for tRNA-specific enzymes and cleavage specificity at the 3′ end of turnip yellow mosaic virus RNA. Nucleic Acids Res. **10:**1947–1962.
29. **Joshi, R. L., H. Faulhammer, F. Chapeville, M. Sprinzl, and A.-L. Haenni.** 1984. Aminoacyl RNA domain of turnip yellow mosaic virus Val-RNA interacting with elongation factor Tu. Nucleic Acids Res. **12:**7467–7478.
30. **Joshi, R. L., J. M. Ravel, and A.-L. Haenni.** 1986. Interaction of turnip yellow mosaic virus Val-RNA with eukaryotic elongation factor EF-1α: search for a function. EMBO J. **5:**1143–1147.
31. **Kohl, R. J., and T. C. Hall.** 1974. Aminoacylation of RNA from several viruses: amino acid specificity and differential activity of plant, yeast and bacterial synthetases. J. Gen. Virol. **25:**257–261.
32. **Koonin, E. V., and V. V. Dolja.** 1993. Evolution and taxonomy of positive-strand RNA viruses: implications of comparative analysis of amino acid sequences. Crit. Rev. Biochem. Mol. Biol. **28:**375–430.
33. **Lahser, F. C., L. E. Marsh, and T. C. Hall.** 1993. Contributions of the brome mosaic virus RNA-3 3′-nontranslated region to replication and translation. J. Virol. **67:**3295–3303.
34. **Lane, L.** 1986. Propagation and purification of RNA plant viruses. Methods Enzymol. **118:**687–696.
35. **Leathers, V., R. Tanguay, M. Kobayashi, and D. R. Gallie.** 1993. A phylogenetically conserved sequence within viral 3′ untranslated RNA pseudoknots regulates translation. Mol. Cell. Biol. **13:**5331–5347.
36. **Meshi, T., T. Ohno, H. Iba, and Y. Okada.** 1981. Nucleotide sequence of a cloned cDNA copy of TMV (cowpea strain) RNA, including the assembly origin, the coat protein cistron, and the 3′ noncoding region. Mol. Gen. Genet. **184:**20–25.
37. **Miller, W. A., J. J. Bujarski, T. W. Dreher, and T. C. Hall.** 1986. Minus strand initiation by brome mosaic virus replicase within the 3′ tRNA-like structure of native and modified RNA templates. J. Mol. Biol. **187:**537–546.
38. **Öberg, B., and L. Philipson.** 1972. Binding of histidine to tobacco mosaic virus RNA. Biochem. Biophys. Res. Commun. **48:**927–932.
39. **Osorio-Keese, M. E., P. Keese, and A. Gibbs.** 1989. Nucleotide sequence of

eggplant mosaic tymovirus genome. Virology **172:**547–554.
40. **Perret, V., C. Florentz, and R. Giegé.** 1990. Efficient aminoacylation of a yeast $tRNA^{Asp}$ transcript with a 5′ extension. FEBS Lett. **270:**4–7.
41. **Pinck, M., and T. C. Hall.** 1978. Aminoacylation properties of eggplant mosaic virus RNA. Separation and association of tRNAs. Virology **88:**281–285.
42. **Pinck, M., P. Yot, F. Chapeville, and H. M. Duranton.** 1970. Enzymatic binding of valine to the 3′ end of turnip yellow mosaic virus RNA. Nature (London) **226:**954–956.
43. **Pleij, C. W. A., J. P. Abrahams, A. van Belkum, K. Rietveld, and L. Bosch.** 1987. The spacial folding of the 3′ noncoding region of aminoacylatable plant viral RNAs, p. 299–316. *In* M. A. Brinton and R. R. Rueckert (ed.), Positive strand RNA viruses. Alan R. Liss, Inc., New York.
44. **Rao, A. L. N., T. W. Dreher, L. E. Marsh, and T. C. Hall.** 1989. Telomeric function of the tRNA-like structure of BMV RNA. Proc. Natl. Acad. Sci. USA **86:**5335–5339.
45. **Rao, A. L. N., and R. I. B. Francki.** 1981. Comparative studies on tomato aspermy and cucumber mosaic viruses. VI. Partial compatibility of genome segments from the two viruses. Virology **114:**573–575.
46. **Rao, A. L. N., and G. L. Grantham.** 1994. Amplification *in vivo* of brome mosaic virus RNAs bearing 3′ noncoding region from cucumber mosaic virus. Virology **204:**478–481.
47. **Rudinger, J., C. Florentz, T. W. Dreher, and R. Giegé.** 1992. Efficient mischarging of a viral tRNA-like structure and aminoacylation of a minihelix containing a pseudoknot: histidylation of turnip yellow mosaic virus RNA. Nucleic Acids Res. **20:**1865–1870.
48. **Sarkar, G., and S. S. Sommer.** 1990. The "megaprimer" method of site-directed mutagenesis. BioTechniques **8:**404–407.
49. **Schaaper, R. M.** 1988. Mechanisms of mutagenesis in the *E. coli* mutator mutD5: role of DNA mismatch repair. Proc. Natl. Acad. Sci. USA **85:**8126–8130.
50. **Schulman, L. H., and H. Pelka.** 1988. Anticodon switching changes the identity of methionine and valine transfer RNAs. Science **242:**765–768.
51. **Swerdlow, H., K. Dew-Jager, and R. F. Gesteland.** 1993. Rapid cycle sequencing in an air thermal cycler. BioTechniques **15:**512–519.
52. **Takamatsu, N., Y. Watanabe, T. Meshi, and Y. Okada.** 1990. Mutational analysis of the pseudoknot region in the 3′ noncoding region of tobacco mosaic virus RNA. J. Virol. **64:**3686–3693.
53. **Tamura, K., H. Himeno, H. Asahara, T. Hasegawa, and M. Shimizu.** 1991. Identity determinants of *E. coli* $tRNA^{Val}$. Biochem. Biophys. Res. Commun. **177:**619–623.
54. **Tsai, C.-H., and T. W. Dreher.** 1991. Turnip yellow mosaic virus RNAs with anticodon loop substitutions that result in decreased valylation fail to replicate efficiently. J. Virol. **65:**3060–3067.
55. **Tsai, C.-H., and T. W. Dreher.** 1992. Second site suppressor mutations assist in studying the function of the 3′ noncoding region of turnip yellow mosaic virus RNA. J. Virol. **66:**5190–5199.
56. **Tsai, C.-H., and T. W. Dreher.** 1993. *In vitro* transcription of RNAs with defined 3′ termini from PCR-generated templates. BioTechniques **14:**58–61.
57. **van Belkum, A., J. Bingkun, K. Rietveld, C. W. A. Pleij, and L. Bosch.** 1987. Structural similarities among valine-accepting tRNA-like structures in tymoviral RNAs and elongator tRNAs. Biochemistry **26:**1144–1151.
58. **Weiland, J. J., and T. W. Dreher.** 1989. Infectious TYMV RNA from cloned cDNA. Effects *in vitro* and *in vivo* of point substitutions in the initiation codons of two extensively overlapping ORFs. Nucleic Acids Res. **17:**4675–4687.
59. **Weiland, J. J., and T. W. Dreher.** 1993. Cis-preferential replication of the turnip yellow mosaic virus RNA genome. Proc. Natl. Acad. Sci. USA **90:**6095–6099.